

# 1 Interferon-gamma promotes iron export in human 2 macrophages to limit intracellular bacterial replication

3 Rodrigo Abreu<sup>1</sup>, Lauren Essler<sup>1</sup>, Pramod Giri<sup>1</sup>, and Fred Quinn<sup>1</sup>,

4 <sup>1</sup>Department of Infectious Diseases, University of Georgia, Athens, Georgia, United States of  
5 America

6 Corresponding author – Fred Quinn, 501 D.W brooks, Athens GA, 30602, [fquinn@uga.edu](mailto:fquinn@uga.edu),  
7 706.542.5790

8

## 9 Abstract

10 Salmonellosis and listeriosis together accounted for more than one third of foodborne  
11 illnesses in the United States and almost half the hospitalizations for gastrointestinal diseases in  
12 2018 while tuberculosis afflicted over 10 million people worldwide causing almost 2 million deaths.  
13 Regardless of the intrinsic virulence differences among *Listeria monocytogenes*, *Salmonella*  
14 *enterica* and *Mycobacterium tuberculosis*, these intracellular pathogens share the ability to  
15 survive and persist inside the macrophage and other cells and thrive in iron rich environments.  
16 Interferon-gamma (IFN- $\gamma$ ) is a central cytokine in host defense against intracellular pathogens  
17 and has been shown to promote iron export in macrophages. We hypothesize that IFN- $\gamma$   
18 decreases iron availability to intracellular pathogens consequently limiting replication in these  
19 cells. In this study, we show that IFN- $\gamma$  regulates the expression of iron-related proteins hepcidin,  
20 ferroportin, and ferritin to induce iron export from macrophages. *Listeria monocytogenes*, *S.*  
21 *enterica*, and *M. tuberculosis* infections significantly induce iron sequestration in human

22 macrophages. In contrast, IFN- $\gamma$  significantly reduces hepcidin secretion in *S. enterica* and *M.*  
23 *tuberculosis* infected macrophages. Similarly, IFN- $\gamma$ -activated macrophages express higher  
24 ferroportin levels than untreated controls even after infection with *L. monocytogenes* bacilli;  
25 bacterial infection greatly down-regulates ferroportin expression. Collectively, IFN- $\gamma$  significantly  
26 inhibits pathogen-associated intracellular iron sequestration in macrophages and consequently  
27 retards the growth of intracellular bacterial pathogens by decreasing iron availability.

28

## 29 **Introduction**

30 In Europe and the US alone, more than three million people live with HIV (1-4) and 15 to 19%  
31 of the population is over 65-years old (5, 6). Thus, these approximately 50 million people have  
32 weakened immune systems and increased risk of serious complications upon infection with self-  
33 resolving pathogens such as *L. monocytogenes* or *S. enterica* (7). Salmonellosis accounts for  
34 38% of all foodborne diseases in the US and the second most commonly reported gastrointestinal  
35 infection in Europe (8-10). Listeriosis reports are less common but have the highest rates of  
36 hospitalization and death among all foodborne illness cases (11, 12). Tuberculosis is leading  
37 cause of death in HIV infected people and is the deadliest infectious disease in the world on its  
38 own (13, 14). In Europe, almost 60,000 new cases of tuberculosis were reported in 2018 (11, 15),  
39 while in the US, almost 8,000 people were afflicted with this disease in 2018 (16).

40 Despite the overall physiological, pathogenic and genetic differences among *L.*  
41 *monocytogenes*, *S. enterica* and *M. tuberculosis*, these pathogens share the ability to survive and  
42 replicate inside non-activated macrophages (17). By inhibiting macrophage antimicrobial  
43 functions, these pathogens evade both innate and adaptive immune responses and persist within  
44 the host for long periods of time (18). Furthermore, these three pathogens are associated with

45 reactivation and recurrent infection in immunocompromised individuals such as the elderly or HIV  
46 infected patients (19-23).

47 IFN- $\gamma$  is a critical cytokine for innate and adaptive immune responses against intracellular  
48 bacteria (24, 25). IFN- $\gamma$  knock-out mice are very susceptible to *L. monocytogenes* (26), *S. enterica*  
49 (27) and *M. tuberculosis* (28) infections. In humans, impaired IFN- $\gamma$  signaling is particularly  
50 associated with increased risk of tuberculosis (29). During the adaptive immune response, IFN- $\gamma$   
51 controls the differentiation CD4<sub>Th1</sub> effector T cells that mediate cellular immunity against  
52 intracellular bacterial infections. Interferon-gamma-activated macrophages possess up-regulated  
53 antigen presentation and increased phagocytosis capabilities, enhanced production of superoxide  
54 radicals, nitric oxide and hydrogen peroxide, and enhanced secretion of pro-inflammatory  
55 cytokines (18, 30). Recently, IFN- $\gamma$  also has been shown to increase ferroportin expression in *S.*  
56 *enterica* infected murine macrophages, promoting iron export and limiting intracellular bacterial  
57 replication (31).

58 Aside from the ability to survive and persist inside non-activated macrophages and other non-  
59 phagocytic cells, *L. monocytogenes*, *S. enterica*, and *M. tuberculosis* also share the ability to  
60 thrive in iron rich environments (32-35). Deletion of iron acquisition genes in these siderophilic  
61 bacteria results in severely attenuated bacterial strains (35, 36), while host iron dysregulation is  
62 greatly associated with worsened disease outcomes with all three of these pathogens (37).

63 In this study we show that IFN- $\gamma$  promotes iron export and efficiently prevents pathogen-  
64 associated intracellular iron sequestration in THP-1 human macrophages during infections with  
65 *L. monocytogenes*, *S. enterica* and *M. tuberculosis* or the attenuated vaccine strain,  
66 *Mycobacterium bovis* BCG. Furthermore, the resulting decrease in intracellular iron availability to  
67 these siderophilic bacteria significantly limits bacterial replication inside the macrophage

68 resembling the effect of iron chelation therapy. The outcome of this work reveals a novel  
69 mechanism by which IFN- $\gamma$  limits intracellular bacterial replication in human macrophages.

## 70 **Results**

### 71 **IFN- $\gamma$ treatment favors iron export in human macrophages**

72 IFN- $\gamma$  has been previously shown to decrease intracellular iron levels and limit *Salmonella*  
73 bacterial replication in mouse macrophages (38). To determine if IFN- $\gamma$  can also modulate iron  
74 regulating genes in human macrophages, human THP-1 differentiated macrophages were treated  
75 with human recombinant IFN- $\gamma$  (200U/ml) and transcriptional expression of the genes for the iron  
76 regulator hepcidin (*HAMP*), iron exporter ferroportin (*SLC40A1*) and intracellular iron storage  
77 protein ferritin (*FTH*) was quantified by qRT-PCR. In agreement with the abovementioned study,  
78 *SLC40A1* transcriptional levels were 2.5-fold higher ( $\pm 0.23$ ,  $p=0.005$ ) 16 hours after IFN- $\gamma$   
79 treatment compared to untreated controls (Fig 1A). Alternatively, transcriptional expression of  
80 *HAMP*, (hepcidin down-regulates ferroportin post-translationally) decreased approximately 70%  
81 ( $p<0.001$ ) after IFN- $\gamma$  treatment (Fig 1B), again biasing towards an iron export phenotype. These  
82 transcriptional data are further supported by the corresponding protein levels assayed using  
83 immunofluorescence in the culture medium (Fig 1C and D). Hepcidin secretion was significantly  
84 decreased (Fig 1D,  $p<0.001$ ) after IFN- $\gamma$  treatment while surface ferroportin was increased (Fig  
85 1C). Interestingly, despite the difference in ferroportin and hepcidin expression levels, IFN- $\gamma$   
86 treatment does not alter transcriptional levels of *FTH* (Fig1E).

87

88 **Fig 1. Interferon-gamma regulates iron-related genes to favor iron export.** A) transcriptional  
89 expression levels of *SLC40A1*, and (B) *HAMP* genes in THP-1 macrophages treated overnight  
90 with 200U/ml IFN- $\gamma$  measured by qRT-PCR and compared to untreated controls. C) Ferroportin

91 protein expression assessed in THP-1 macrophages treated as in A. D) Heparin secretion levels  
92 in THP-1 macrophages treated as in B (magnification = 63X). E) Transcriptional expression levels  
93 of the *FTH* gene in THP-1 macrophages treated as in A and B. \*\* $p < 0.01$ , \*\*\* $p < 0.001$ . All data  
94 were from three independent experiments.

## 95 **Siderophilic bacteria manipulate host iron-related proteins to favor** 96 **intracellular iron sequestration**

97 Intracellular siderophilic bacteria such as *M. tuberculosis*, *M. bovis* BCG, *L. monocytogenes*  
98 or *S. enterica* prominently activate Toll-like receptor signaling (25). Interaction and activation of  
99 Toll-like receptors expressed by macrophages induce intracellular iron sequestration both through  
100 increased hepcidin secretion and decreased ferroportin expression (39). To test if these  
101 siderophilic organisms can manipulate host iron-related proteins in the macrophage, THP-1  
102 differentiated macrophages were infected with *M. tuberculosis*, *M. bovis* BCG, *L. monocytogenes*,  
103 or *S. enterica*, and hepcidin secretion was quantified by ELISA at the peaks of infection (24 hours  
104 for *M. tuberculosis* and *M. bovis* BCG, eight hours for *L. monocytogenes* and 16 hours for *S.*  
105 *enterica*). Upon infection, both *M. tuberculosis* and *M. bovis* BCG infected macrophages secreted  
106 significantly more hepcidin than respective uninfected controls, 48 hours and 24 hours after  
107 infection, respectively (mean difference was  $88.6 \pm 2.8$  pg/ml and  $76.2 \pm 1.2$  pg/ml, respectively,  
108  $p < 0.0001$ ). This represents an approximate three-fold increase. In the same way, infection with  
109 *S. enterica* resulted in increased hepcidin secretion, in agreement with our previous report  
110 suggesting that TLR-4 activation is responsible for hepcidin expression in macrophages during  
111 infection (39) (Fig 2A).

112 Alternatively, *L. monocytogenes* infection had no impact on hepcidin secretion (Fig 2A),  
113 although it did result in direct ferroportin gene down-regulation, independent of hepcidin  
114 expression (Fig 2B and C). *Listeria monocytogenes* infected macrophages express lower levels

115 of surface ferroportin compared to uninfected controls (Fig 2B), a 60% decrease measured by  
116 mean fluorescence intensity. To confirm that infection with *L. monocytogenes* bacteria down-  
117 regulates ferroportin through a hepcidin-independent mechanism, we silenced hepcidin  
118 expression through hepcidin gene specific lentiviral ShRNA (S1 Fig). Scramble negative controls  
119 (ShScram) and lentiviral ShRNA-silenced expression of the hepcidin gene (ShHAMP) in THP-1  
120 differentiated macrophages were infected with *L. monocytogenes* bacilli; these infected cells  
121 expressed similar surface ferroportin levels (Fig 2C and S2) supporting the hypothesis that this  
122 pathogen can promote intracellular iron sequestration, through direct ferroportin down-regulation.

123

124 **Fig 2. Intracellular pathogens modulate iron-related proteins to favor intracellular iron**  
125 **sequestration in macrophages.** A) Hepcidin secretion from THP-1 macrophages after infection  
126 with *M. tuberculosis* (24 hours), *M. bovis* BCG (24 hours), *L. monocytogenes* (eight hours) or *S.*  
127 *enterica* (16 hours) bacilli. B) Ferroportin levels in THP- 1 macrophages eight hours post-infection  
128 with *L. monocytogenes* (magnification = 40X). C) Ferroportin expression in hepcidin silenced  
129 THP-1 macrophages eight hours post infection with *L. monocytogenes*. Hepcidin gene silencing  
130 in THP-1 cells was achieved by lentiviral based shRNA transduction and Scramble short hairpin  
131 RNAs (ShScram) were used as a negative control (magnification = 40X). \*\*\* $p < 0.001$ . All data  
132 were from three independent experiments.

### 133 **Pathogen-associated intracellular iron sequestration promotes** 134 **intracellular replication**

135 Intracellular bacterial pathogens modulate macrophage iron-related proteins to favor iron  
136 sequestration (Fig 2). We subsequently determined if *M. bovis* BCG, *L. monocytogenes* or *S.*  
137 *enterica* infected macrophages have increased iron content compared to uninfected controls by

138 Prussian Blue iron staining. Uninfected activated macrophages had low iron retention with  
139 minimal iron staining (Fig 3A). However, upon infection with any of the above-mentioned  
140 siderophilic bacteria, macrophages had increased intracellular iron levels as observed by  
141 increased blue granules (Fig 3B-D). This observation was reversible with the addition of IFN- $\gamma$ .  
142 When macrophages were activated with IFN- $\gamma$  before infection with *M. bovis* BCG, *L.*  
143 *monocytogenes* or *S. enterica*, intracellular iron levels significantly decreased, resembling those  
144 of uninfected cells (Fig 3E-G). Interestingly, infections with the three bacterial strains generated  
145 different iron staining patterns: *L. monocytogenes* and *M. bovis* BCG infected macrophages had  
146 increased intracellular iron levels, but in a similar pattern as uninfected cells (small blue granules  
147 dispersed in the cytoplasm) (Fig 3A-C), while *S. enterica* infected macrophages generated large  
148 iron stained granules in the cytoplasm (Fig 3D).

149

150 **Fig 3. Interferon-gamma treatment decreases pathogen-associated intracellular iron**  
151 **sequestration.** A) Intracellular iron levels assessed by Prussian Blue staining in untreated and  
152 IFN- $\gamma$  activated THP-1 macrophages, and (B-D) infected with three siderophilic bacteria  
153 (magnification = 100X). Percentage total area of Prussian Blue (PB) pixels in macrophages after  
154 infection with (E) *L. monocytogenes*, (F) *M. bovis* BCG, or (G) *S. enterica* with or without IFN- $\gamma$   
155 treatment. \* $p < 0.05$ , \*\* $p < 0.01$ , \*\*\* $p < 0.0001$ .

156 Iron dysregulation is associated with a poorer disease outcome upon infection with  
157 siderophilic bacteria such as *M. tuberculosis*, *L. monocytogenes* and *S. enterica* (40).  
158 Alternatively, iron chelation has proven to be an effective therapy *in vitro* and *in vivo* against some  
159 of these siderophilic pathogens (41). To evaluate if increased intracellular iron sequestration was  
160 essential for bacterial replication, we infected THP-1 differentiated macrophages with *M.*  
161 *tuberculosis*, *L. monocytogenes* and *S. enterica* bacteria in the presence of the iron chelators

162 deferoxamine (DFO) or deferiprone (DFP) and intracellular replication was assessed using the  
163 gentamicin protection assay. DFO was chosen for *M. tuberculosis* infection as an injectable  
164 chelator which has been previously validated for use with *Mycobacteria* (42), while DFP was used  
165 for *L. monocytogenes* and *S. enterica* infections as this oral human therapeutic chelator is more  
166 physiologically relevant for gastrointestinal pathogens. As expected, iron chelation significantly  
167 decreased intracellular replication of *M. tuberculosis* (90% less 72 hours post-infection, S3C Fig),  
168 *L. monocytogenes* (72% less eight hours post-infection, S3D Fig) and *S. enterica* (89% less 16  
169 hours post-infection, S3E Fig).

## 170 **Interferon-gamma prevents pathogen induced iron modulation in** 171 **macrophages**

172 Interferon-gamma treatment and infection with various intracellular pathogens have opposing  
173 effects on macrophage survival (Fig 1 and 2). Thus, IFN- $\gamma$  treatment was assessed for its ability  
174 to prevent iron retention in macrophages infected with *M. bovis* BCG, *L. monocytogenes* or *S.*  
175 *enterica* bacteria. THP-1 activated macrophages were treated with 200U/ml human recombinant  
176 IFN- $\gamma$  overnight and infected with the various species of intracellular bacteria. At different time  
177 points after infection, ferroportin levels were assessed by immunofluorescence and hepcidin  
178 secretion by ELISA. Similar to what was observed with uninfected macrophages (Fig 1), IFN- $\gamma$   
179 treatment increased ferroportin expression in THP-1 macrophages infected with *L.*  
180 *monocytogenes* (Fig 4A), *M. bovis* BCG (Fig 4B), and *S. enterica* (Fig 4C). MFI quantification  
181 revealed that IFN- $\gamma$  treatment significantly increased ferroportin expression by 60% and 74% for  
182 *L. monocytogenes* and *S. enterica*, respectively (S4 Fig).

183 Additionally, IFN- $\gamma$  also decreases hepcidin secretion in the culture supernatants of *L.*  
184 *monocytogenes* (mean difference 37.9 $\pm$ 1.5 pg/ml) and *M. bovis* BCG (mean difference 50.9 $\pm$ 1.5  
185 pg/ml) infected macrophages at eight and 24 hours post-infection, respectively (Fig 4D and E).



186 Surprisingly, IFN- $\gamma$  only marginally inhibits hepcidin secretion from *S. enterica* infected  
187 macrophages to levels still significantly higher than uninfected controls (mean difference  
188  $47.2 \pm 1.97$  pg/ml,  $p < 0.001$ ) (Fig 4F).

189

190 **Fig 4. Interferon-gamma prevents pathogen associated iron modulation in macrophages.**

191 A) Ferroportin expression in IFN- $\gamma$ -activated (200U/ml) macrophages eight hours post infection  
192 with *L. monocytogenes*, (B) 48 hours post infection with *M. bovis* BCG, or (C) 16 hours post  
193 infection with *S. enterica* (magnification = 40X). D) Hepcidin secretion in the culture supernatants  
194 of IFN- $\gamma$ -activated macrophages eight hours post infection with *L. monocytogenes*, (E) 24 hours  
195 post infection with *M. bovis* BCG, or (F) 16 hours post infection with *S. enterica*. \*\* $p < 0.01$ ,  
196 \*\*\* $p < 0.001$ . All data were from three independent experiments.

197 **Interferon-gamma limits intracellular *Salmonella* and *Mycobacterium***  
198 **bacterial replication in macrophages through hepcidin inhibition**

199 Treatment with IFN- $\gamma$  counteracts pathogen modulation of iron-regulating genes (Fig 4)  
200 favoring iron export. It has been previously reported that IFN- $\gamma$  limits iron availability to intracellular  
201 pathogens through up-regulation of ferroportin leading to decreased bacterial replication (31). To  
202 assess if hepcidin inhibition and increased ferroportin expression would translate to decreased  
203 intracellular bacterial replication, ShHAMP THP-1 macrophages were infected and intracellular  
204 bacterial replication assessed using the gentamicin protection assay. As observed with IFN- $\gamma$   
205 treatment, hepcidin silencing leads to increased ferroportin expression in uninfected  
206 macrophages favoring iron export (Fig 1B). Upon infection with *S. enterica*, ShHAMP THP-1  
207 macrophages showed significantly decreased intracellular bacterial replication than respective  
208 negative scramble controls (ShScram) (90% decrease) at 16 hours post infection (Fig 5A). A

209 similar impact (70% decrease) in intracellular bacterial replication was observed at 48 and 72  
210 hours post infection with *M. tuberculosis* (Fig 5B). However, *L. monocytogenes* replication was  
211 not altered in ShHAMP THP-1 macrophages, suggesting that *Listeria*-mediated iron sequestration  
212 is hepcidin-independent (Fig 5C).

213 Interferon-gamma limits intracellular bacterial replication in macrophages through activation  
214 of multiple anti-microbial mechanisms (43). To confirm that the concentrations tested in this work  
215 inducing iron export also reduced intracellular bacterial replication, we treated THP-1  
216 differentiated macrophages with 200U/ml IFN- $\gamma$  before infection with *L. monocytogenes*, *S.*  
217 *enterica* or *M. tuberculosis* and quantified intracellular bacterial burden in a gentamicin protection  
218 assay. *L. monocytogenes*, *S. enterica* and *M. tuberculosis* infected macrophages had significantly  
219 decreased intracellular bacterial burdens after IFN- $\gamma$  treatment at 8, 16 and 24 hours post  
220 infections, respectively (Fig 5D - F). In *S. enterica* or *M. tuberculosis*-infected macrophages, IFN- $\gamma$   
221 has a significant impact on intracellular bacterial counts 16 and 48 hours post-infection, where it  
222 translates into a 90% decrease in bacterial numbers compared to untreated controls (Fig 5E and  
223 D). Similarly, IFN- $\gamma$  treatment results in an 80% decrease in *L. monocytogenes* intracellular  
224 bacterial numbers six hours post-infection (Fig 5F).

225

226 **Fig 5. Hepcidin inhibition limits intracellular *M. tuberculosis* and *S. enterica* bacterial**  
227 **replication in macrophages.** *Salmonella enterica* (A), *M. tuberculosis* (B) and *L. monocytogenes*  
228 (C) intracellular burden in ShHAMP THP-1 macrophages and respective ShScram controls.  
229 *Salmonella enterica* (D), *M. tuberculosis* (E) and *L. monocytogenes* (F) intracellular burden in  
230 IFN- $\gamma$ -activated macrophages (200U/ml) and respective untreated controls. \* $p < 0.05$ , \*\*\* $p < 0.001$ .  
231 All data were from three independent experiments.

## 232 Discussion

233 The host immune response to intracellular bacteria is a complex network of pro- and anti-  
234 inflammatory mediators assuring efficient bacterial killing with minimal tissue damage (18). In  
235 contrast, bacterial persistence is a fine tuning of virulence factors that coordinate bacterial survival  
236 within the host with minimal activation of the surveillance immune system (17). *Mycobacterium*  
237 *tuberculosis*, *L. monocytogenes* and *S. enterica* serovar Typhimurium are three intracellular  
238 bacterial species that persist in macrophages and efficiently avoid the host immune system.  
239 Despite the varied factors involved in bacterial survival and replication inside the macrophage,  
240 these three pathogens share the ability to avoid or inhibit macrophage anti-microbial functions  
241 such as phagosome maturation, phagolysosome fusion or induction of nitric and oxygen reactive  
242 species (17). In contrast, IFN- $\gamma$  macrophage activation promotes intracellular bacterial killing  
243 through direct induction of the abovementioned antimicrobial mechanisms (44). In this study, we  
244 describe a novel mechanism by which IFN- $\gamma$  limits intracellular bacterial replication in  
245 macrophages. In human macrophages, IFN- $\gamma$  promotes iron export and efficiently prevents  
246 pathogen-associated intracellular iron sequestration. The consequent decrease in intracellular  
247 iron availability to these siderophilic bacterial pathogens significantly limits their replication inside  
248 the macrophage.

249 Iron is a crucial micronutrient to all forms of life with important biological functions. This metal  
250 is a component of molecules involved in sensing, transporting and storing oxygen, and of  
251 enzymes involved in oxidation and reduction of substrates during energy production, intermediate  
252 metabolism, and the generation of reactive oxygen or nitrogen species for host defense. During  
253 infection with siderophilic bacteria, decreased iron availability greatly impedes intracellular  
254 bacterial replication (40). Pathogen-associated intracellular iron regulation in macrophages is  
255 dependent on TLR signaling and mediated through two independent and redundant mechanisms  
256 regulating the iron-related proteins hepcidin and ferroportin (39). Secreted hepcidin binds to  
257 surface ferroportin of mammalian cells to induce its internalization and degradation, resulting in

258 decreased iron export (45). While TLR-4, TLR-7 and TLR-8 signaling induces hepcidin secretion,  
259 TLR-1, TLR-2 and TLR-6 activation significantly inhibits ferroportin expression in THP-1 human  
260 macrophages (39).

261 In this study we show that *L. monocytogenes* infection promotes intracellular iron  
262 sequestration in macrophages through ferroportin downregulation, independent of hepcidin  
263 expression (Fig 2). These results are consistent with predominant TLR-2 activation during *L.*  
264 *monocytogenes* infection (46), and in support of previously published results (47) where *L.*  
265 *monocytogenes* significantly decreases ferroportin expression through a hepcidin-independent  
266 mechanism. IFN- $\gamma$  treatment significantly increases ferroportin expression in THP-1 macrophages  
267 even after *L. monocytogenes* infection (Fig 3A) inhibiting *Listeria*-associated intracellular iron  
268 sequestration.

269 Increased hepcidin expression has been shown to promote intracellular *M. bovis* BCG  
270 replication (39, 48), and HIV replication is augmented in hepcidin-treated macrophages (49).  
271 *Salmonella enterica* significantly induces hepcidin expression consistent with TLR-4 signaling (Fig  
272 2), whereas *M. tuberculosis* and *M. bovis* BCG, which activate both TLR-2 and TLR-4, promote  
273 intracellular iron sequestration through hepcidin-independent and dependent mechanisms (Fig  
274 3). In this study, it was observed that IFN- $\gamma$  treatment inhibits hepcidin secretion in human  
275 macrophages (Fig 1) and significantly decreases pathogen-induced hepcidin secretion during *M.*  
276 *bovis* BCG or *S. enterica* infection (Fig 4), subsequently reducing intracellular iron sequestration  
277 in infected macrophages (Fig 3).

278 *M. bovis* BCG was used as model for *M. tuberculosis* in several assays that required analysis  
279 at biosafety level 2 (Fig 3 and 4). However, we feel *M. bovis* BCG is an adequate substitute for  
280 these studies and the data generated here are comparable to *M. tuberculosis* for a number of  
281 reasons: It is well known that *M. bovis* BCG maintains a high genetic homology and similar cell

282 wall composition to *M. tuberculosis* (50, 51), and it has been observed here (Fig 1) and in other  
283 studies (52-54) that within the 24-48 hour infection times used in this study, no differences in the  
284 bacterial replication rates, trafficking patterns, or host cell viability rates are observed between *M.*  
285 *tuberculosis* and *M. bovis* BCG infected cell lines. These common traits at least in the earliest  
286 stages of infection allow *M. bovis* BCG to extrinsically activate TLR signaling and induce hepcidin  
287 secretion and intracellular iron retention much like *M. tuberculosis* (Fig 2 and 3). All of these  
288 common traits are important when considering their contributions to maximizing vaccine efficacy  
289 for *M. bovis* BCG.

290 Ferroportin overexpression in murine macrophages is able to severely impair *S. enterica*  
291 growth (55). Similarly, reducing hepcidin gene expression in ShHAMP THP-1 cells reduces *S.*  
292 *enterica* replication, showing that IFN- $\gamma$ -mediated hepcidin down-regulation alone can  
293 significantly impact intracellular replication (Fig 5). Moreover, sodium phenylbutyrate, a strong  
294 hepcidin inhibitor in macrophages (unpublished data) has been shown to significantly inhibit *S.*  
295 *enterica* growth *in vivo* (56). In contrast, *L. monocytogenes* intracellular bacterial burden remains  
296 unaltered in ShHAMP macrophages, indicating that IFN- $\gamma$ -induced ferroportin expression is an  
297 important factor limiting bacterial growth during *L. monocytogenes* infection (Fig 5).

298 Bacteria possess a myriad of mechanisms to scavenge the host iron pool, and the three  
299 pathogens used in this study utilize different iron scavenging strategies (57). *Mycobacterium*  
300 *tuberculosis* siderophores, mycobactin and carboxymycobactin, efficiently recruit and scavenge  
301 iron in the phagosome (58). Carboxymycobactin is the major iron-chelator for both free and  
302 protein-bound iron in the macrophage phagosome and cytoplasm (58, 59), while surface  
303 mycobactin acts as a membrane chelator and iron-transporter recovering iron from  
304 carboxymycobactin and host ferritin (60). In macrophages, ferritin mostly localizes to the nucleus  
305 with minimal cytoplasmic distribution (61), and *M. bovis* BCG-infected macrophages present  
306 increased iron retention in the nucleus with some diffuse iron distribution in the cytoplasm (Fig 3).

307 Iron-loaded ferritin has been previously shown to be efficiently recruited to the phagosome and  
308 utilized by *M. tuberculosis* (60). Future studies may explore the impact of IFN- $\gamma$  in intracellular iron  
309 distribution within the macrophage and its accessibility to mycobacteria.

310 *Salmonella enterica* inhibits phagolysosome fusion, and persists and replicates inside the  
311 immature phagosome compartment (62). During infection, efficient control of intra-phagosome  
312 iron levels by the phagosomal iron exporter NRAMP is essential to limit bacterial replication (38,  
313 63). *Salmonella enterica* iron acquisition strategies are very similar to other Gram-negative  
314 bacteria and mostly dependent on the ferric siderophores enterochelin and salmochelin (34, 64).  
315 These siderophores scavenge iron from the host proteins transferrin and lactoferrin, with the iron-  
316 laden siderophores then transported through bacterial outer-membrane receptors IroN and FepA  
317 (64, 65). Besides this mechanism, *S. enterica* also can utilize heme-iron sources inside the  
318 phagosome, although this seems to be more prominent during infection of hemophagocytic  
319 macrophages (65). Consistent with the use of intra-phagosomal iron sources, *S. enterica* infected  
320 macrophages have localized iron aggregates (Fig 3) possibly associated with immature  
321 phagosomes where the bacteria persist. Although iron supplementation decreases bacterial  
322 survival during early stages of infection, probably through increased ROS generation, at 16 hours  
323 post infection increased iron levels are detrimental for the host and facilitate bacterial replication  
324 (S5 Fig). This supports the hypothesis of pathogen-mediated iron recruitment and accumulation  
325 in the phagosome. This accumulated iron then counteracts NRAMP iron export from the  
326 phagosome at later stages of infection which is needed for efficient bacterial clearance. Aside  
327 from confirming iron localization to the phagosome, future studies may assess how iron gets  
328 recruited to this compartment and how NRAMP impacts iron distribution in the macrophage.

329 Siderophore synthesis genes are absent in the *L. monocytogenes* genome, therefore heme-  
330 bound iron is proposed as the major iron source utilized by this pathogen during macrophage  
331 infection (66). Phagosomal activation of the pore-forming protein listeriolysin-O leads to bacterial

332 escape from the phagosome to the cytoplasm (24, 67). Once in the cytoplasm expression of the  
333 ferrochrome ABC transporters *hupCGD* (*Imo2429/30/31*) enhances iron acquisition from heme-  
334 proteins (33, 66). The diffuse cytoplasmic distribution of intracellular iron in *L. monocytogenes*  
335 infected macrophages (Fig 3) may represent an increase in heme-proteins which can be efficiently  
336 used as an iron source. In the future it would be interesting to identify the major heme-proteins  
337 targeted by *L. monocytogenes* for iron scavenging and assess the impact of IFN- $\gamma$  signaling on  
338 the expression of these same proteins.

339 Hepcidin was first identified as an antimicrobial peptide utilized by the host cell during  
340 infection with extracellular pathogens; this work has been extensively reported (68, 69). As with  
341 lactoferrin, hepcidin efficiently decreases extracellular iron availability to pathogens such as *Vibrio*  
342 *cholerae* (63, 70). However, during infection with intracellular pathogens hepcidin-mediated  
343 intracellular iron sequestration in macrophages is deleterious for the host and facilitates bacterial  
344 replication (49, 55, 71, 72). Furthermore, hepcidin has been reported to play an anti-inflammatory  
345 role during chronic infections which could further dampen an effective immune repose against  
346 persistent intracellular pathogens (73, 74).

## 347 **Conclusions**

348 Interferon- $\gamma$  is an important cytokine in both the innate and adaptive immune responses  
349 against intracellular pathogens. This cytokine upregulates major histocompatibility complex class  
350 I and class II antigen presentation, and contributes to macrophage activation by increasing  
351 phagocytosis and priming the production of pro-inflammatory cytokines and potent antimicrobials,  
352 including superoxide radicals, nitric oxide, and hydrogen peroxide (43). Interferon-gamma also  
353 controls the differentiation CD4<sub>Th1</sub> effector T cells which mediate cellular immunity against  
354 intracellular bacterial infections. The role of IFN- $\gamma$  in regulating intracellular iron availability for *S.*  
355 *enterica* has been previously reported, but with conflicting results. While IFN- $\gamma$ -mediated nitric

356 oxide production significantly increased ferroportin expression in murine macrophages which  
357 significantly contributed to limiting intracellular bacterial replication (43), IFN- $\gamma$  treatment has also  
358 been shown to upregulated hepcidin expression in a murine macrophage *M. tuberculosis* infection  
359 model (75). This report contradicts our observations that describe a positive outcome where IFN- $\gamma$   
360 strongly promotes iron export in human macrophages through increased ferroportin expression  
361 and decreased hepcidin secretion. The consequent decrease in intracellular iron availability  
362 severely limits replication of three different bacterial pathogens, *L. monocytogenes*, *S. enterica*  
363 and *M. tuberculosis*. Thus, our study elucidates a novel mechanism by which IFN- $\gamma$  controls  
364 intracellular bacterial replication and exposes iron dysregulation as an important factor of innate  
365 immunity against these pathogens.

## 366 **Materials and methods**

### 367 **Cell culture and macrophage differentiation**

368 The THP-1 monocytic cell line was obtained from ATCC (#TIB-202) and maintained in  
369 complete RPMI with 2mM glutamine and supplemented with 10% heat inactivated fetal bovine  
370 serum (C-RPMI). For differentiation into a macrophage-like phenotype, cells were resuspended  
371 at a concentration of  $8 \times 10^5$  per ml, treated with 50nM phorbol 12-myristate 13-acetate (PMA) for  
372 24 hours and rested overnight in C-RPMI with 100 $\mu$ M ferric ammonium citrate (FeAC) and  
373 200U/ml of human recombinant IFN- $\gamma$  (R&D Systems, MN USA) unless otherwise stated.

### 374 **Hepcidin silencing**

375 The THP-1 monocytic cell line was transduced with gene-silencing Short-hairpin RNA  
376 (ShRNA) lentiviral particles (Santa Cruz Biotech, TX, USA). Briefly,  $2 \times 10^3$  THP-1 cells were  
377 grown in v-bottom 96-well plates with Hepcidin-specific ShRNA lentiviral particles or respective



378 scramble control at a multiplicity of infection of 10 with 5 µg/ml polybrene. Cells were centrifuged  
379 at 900xg for 30 minutes to increase contact and incubated overnight at 37°C with 5% CO<sub>2</sub>. Cells  
380 were then centrifuged for 5 minutes at 400xg, resuspended in C-RPMI, monitored for viability and  
381 sequentially expanded to 48-wells in C-RPMI. When monolayers reached 50% confluency in 48  
382 well plates, stably transduced cells were selected with 1 µg/ml puromycin and expanded in T75  
383 flasks, before storage in liquid nitrogen. Thawed aliquots were passaged once before selection  
384 with puromycin.

### 385 **Bacterial strains and infection**

386 The strains used in this study were *M. bovis* BCG (Pasteur), and *M. tuberculosis* (Erdman)  
387 kindly provided by Dr. Jeffery Cox (UC Berkley, CA, USA). *Listeria monocytogenes* was acquired  
388 from ATCC (#15313; VA USA) and clinical isolate *Salmonella enterica* serovar Typhimurium was  
389 kindly provided by Dr. Mary Hondalus (UGA, GA USA). Mycobacteria were grown to an OD<sub>600</sub> ≈  
390 0.8a.u. in Middlebrook 7H9 medium supplemented with Albumin Dextrose Catalase (ADC), 5%  
391 glycerol and 0.5% Tween 80. Frozen stocks were prepared in 20% glycerol 7H9 medium (v/v)  
392 and maintained at -80°C. *Listeria monocytogenes* and *S. enterica* were grown to an OD<sub>600</sub> ≈  
393 0.8a.u. in brain-heart infusion (BHI) or Luria-Bertani broth, respectively. Frozen stocks were made  
394 in the respective media with 20% glycerol (v/v) and stored at -80°C. To test viability of the frozen  
395 stocks, colony forming units/ml were determined by serial dilution and plating of the thawed  
396 suspensions on the respective agar media three weeks after freezing. Before infection, *M. bovis*  
397 BCG or *M. tuberculosis* bacilli were passed through a 21G syringe and opsonized for two hours  
398 in RPMI with 10% non-heat inactivated horse serum at 37°C with gentle rocking.

399 For mycobacterial infections, 3X10<sup>5</sup> PMA-differentiated THP-1 macrophages were incubated  
400 in C-RPMI with opsonized bacilli in 48 well plates. Infections were performed using a multiplicity  
401 of infection of five to 10 bacilli per cell, for two hours at 37°C with 5% CO<sub>2</sub>. After internalization,

402 macrophages were washed twice with PBS and left on C-RPMI with 50 µg/ml gentamicin and 200  
403 U/ml IFN-γ throughout infection. For intracellular bacterial burden quantification, host cells were  
404 lysed at indicated time points with 0.1% TritonX-100 for 10 minutes and serial dilutions plated in  
405 7H10 agar medium. Bacterial colonies were counted twice after 19 to 23 day incubations at 37°C.

406 For *L. monocytogenes* and *S. enterica* infections, macrophages were seeded as described  
407 above and incubated with non-opsonized bacteria in C-RPMI for one hour at 37°C with 5% CO<sub>2</sub>.  
408 After internalization, the intracellular bacterial burden was determined as described above for  
409 mycobacterial infections but instead using BHI or LB agar plates after 24 hours incubation at  
410 37°C.

## 411 RNA extraction and real-time PCR

412 Total cellular RNA from 1X10<sup>6</sup> THP-1 macrophages was extracted with TRIzol (Invitrogen,  
413 Thermo Fisher Scient. MA USA) following the manufacturer's protocol and reverse transcribed  
414 into cDNA using a SuperscriptIII First strand cDNA synthesis Kit (Invitrogen, Thermo Fisher  
415 Scientific. MA USA) with poly dT<sub>20</sub> primers. Quantitative PCR (qPCR) was performed using Bio-  
416 Rad IQ SYBR green supermix (Bio-Rad, CA USA) in a iQ™5 Real-Time PCR Detection System.  
417 All values were normalized against reference gene *GAPDH* ( $\Delta\text{CT} = \text{CT} [\text{target}] - \text{CT} [\text{reference}]$ ).  
418 Fold change in expression was calculated as  $2^{-\Delta\Delta\text{CT}}$ , where  $\Delta\Delta\text{CT} = \Delta\text{CT} (\text{test sample}) - \Delta\text{CT}$   
419 (control). The primer sequences for the genes examined were the following: human *HAMP*,  
420 forward, 5'-GGATGCCCATGTTCCAGAG-3'; reverse, 5'-AGCACATCCCACACTTTGAT-3';  
421 human *GAPDH*, forward, 5'-GCCCTCAACGACCACTTTGT -3'; reverse, 5'-  
422 TGGTGGTCCAGGGGTCTTAC- 3', human *SLC40A1*, forward, 5'-  
423 CACAACCGCCAGAGAGGATG-3'; reverse, 5'-ACCAGAAACACAGACACCGC-3'; Human  
424 *FTH*, forward, 5'-AGAACTACCACCAGGACTCA-3'; reverse, 5'-  
425 TCATCGCGGTCAAAGTAGTAAG-3'.

## 426 **Hepcidin secretion quantification**

427 Hepcidin levels in culture supernatants were determined using human hepcidin DuoSet  
428 ELISA Kit (R&D Systems, MN, USA), per manufacture's recommendations.

## 429 **Immunofluorescence microscopy**

430 Anti ferroportin and anti-hepcidin antibodies for ferroportin and hepcidin detection were kindly  
431 provided by Dr. Tara Arvedson, and immunofluorescence staining was performed as previously  
432 described (76). Briefly,  $2 \times 10^5$  THP-1 macrophages were grown and differentiated in eight or 16  
433 well chamber microscopy slides and infected as described above, fixed with 4%  
434 paraformaldehyde (PFA), and permeabilized with 0.1% Triton X-100. For ferroportin staining, cells  
435 were incubated with 2  $\mu\text{g/ml}$  mouse antibody diluted in C-RPMI overnight. For detection, cells  
436 were incubated with 2  $\mu\text{g/ml}$  goat anti-mouse alexa-fluor-488 (Invitrogen, Thermo Fisher Scient.  
437 MA USA) at 4°C for two hours. Cells were counterstained with DAPI. For hepcidin staining, cells  
438 were infected, fixed and permeabilized as described above, and stained with 2  $\mu\text{g/ml}$  mouse anti-  
439 hepcidin antibody overnight at 4°C. Slides were imaged in a Zeiss Axiovert 200M microscope at  
440 40X and 63X and images acquired with AxioCam MRm grey scale camera.

## 441 **Prussian Blue for iron staining**

442 THP-1 macrophages were grown to  $4 \times 10^5$  cells per well in 8 well chamber microscopy slides  
443 and differentiated as described above. After infection, cells were fixed with 4% formaldehyde in  
444 PBS for 10 minutes at room temperature, washed with PBS and stained twice with a 4%  
445 hydrochloric acid and 4% potassium ferrocyanide (1:1 v/v) solution of for 25 minutes (Polysciences  
446 Prussian Blue stain kit, PA USA). After washing with PBS, cells were counterstained with filtered  
447 1% Nuclear Fast red solution for 5 to 10 minutes, washed gently with PBS and water, and  
448 mounted and imaged using an Olympus Bx41 microscope. Images were acquired with an

449 Olympus DP71 color camera using 20X, 40X and 100X lenses, and processed with cellSens  
450 v1.14.

## 451 **Image analysis**

452 Image analysis and mean pixel fluorescence intensity were determined with Zeiss Axiovision  
453 Rel 4.8.1 software. Co-localization and Prussian Blue staining were quantified with image J 1.51K  
454 software. Grey scale images were converted to binary files for automatic shape analysis. Protein-  
455 protein co-localization was determined by double positive pixel areas.

456 Prussian Blue staining was quantified in 20x color image thresholds for background and  
457 determined as percentage of blue pixel area over total pixel area averaged from at least four  
458 different fields from three independent experiments.

## 459 **Statistics**

460 All data are presented as means  $\pm$  SD. Statistical significance differences between groups were  
461 determined using Student's *t* test with GraphPad Prism software (CA, USA).

## 462 **Acknowledgments**

463 We thank Dr. Tara Arvedson (Amgen Inc., CA, USA) for providing ferroportin monoclonal  
464 antibodies. We also thank Shelly Helms for technical assistance in several parts of this project.

## 465 **Funding sources**

466 This work was supported in part by an endowment from the University of Georgia Athletic  
467 Association (F. D. Q.) and Fulbright PhD Scholarship (R.A. 11/278).

## 468 **Conflict-of-interest**

469 The authors have no conflict of interest to declare.

## 470 **Authorship**

471 Contribution: R.A. designed experiments, interpreted data, prepared figures and wrote the  
472 manuscript; L. E. performed experiments, prepared figures, and helped write the manuscript; F.Q  
473 provided guidance, intellectual input, helped write the manuscript and reviewed the manuscript;  
474 P.G. provided guidance, intellectual input, helped write the manuscript and reviewed the  
475 manuscript.

## 476 **References**

- 477
- 478 1. CDC. HIV/AIDS [Available from: <https://www.cdc.gov/hiv/default.html>].
  - 479 2. WHO. HIV [Available from: <http://www.who.int/hiv/en/>].
  - 480 3. ECDC/WHO. HIV/AIDS surveillance in Europe. 2016.
  - 481 4. CDC. Today's HIV/AIDS epidemic 2016.
  - 482 5. Bureau USC. USA aging population [Available from:  
483 <https://www.census.gov/quickfacts/fact/table/US/PST045216>].
  - 484 6. Eurostat. EU population structure [Available from: [http://ec.europa.eu/eurostat/statistics-](http://ec.europa.eu/eurostat/statistics-explained/index.php/Population_structure_and_ageing)  
485 [explained/index.php/Population\\_structure\\_and\\_ageing](http://ec.europa.eu/eurostat/statistics-explained/index.php/Population_structure_and_ageing)].
  - 486 7. USDA. Food safety for people with HIV/AIDS. 2011.
  - 487 8. ECDC. Salmonellosis [Available from: <https://ecdc.europa.eu/en/salmonellosis>].
  - 488 9. ECDC. Food and waterborne diseases and zoonoses. 2014.
  - 489 10. CDC. Foodborne Diseases Active Surveillance Network (FoodNet) 2015 Surveillance  
490 Report. 2017.
  - 491 11. ECDC. Annual Epidemiological Report 2014: Listeriosis. 2016.
  - 492 12. ECDC. Listeriosis [Available from: <https://ecdc.europa.eu/en/listeriosis>].
  - 493 13. WHO. Tuberculosis [Available from:  
494 <http://www.who.int/immunization/diseases/tuberculosis/en/>].
  - 495 14. CDC. Tuberculosis [Available from: <https://www.cdc.gov/tb/default.htm>].

- 496 15. ECDC. Tuberculosis 2014 report. 2015.
- 497 16. CDC. Reported Tuberculosis in the United States, 2015. 2016.
- 498 17. Monack DM, Mueller A, Falkow S. Persistent bacterial infections: the interface of the  
499 pathogen and the host immune system. *Nat Rev Microbiol.* 2004;2(9):747-65.
- 500 18. Kaufmann SH. Immunity to intracellular bacteria. *Annu Rev Immunol.* 1993;11:129-63.
- 501 19. Decker CF, Simon GL, DiGioia RA, Tuazon CU. *Listeria monocytogenes* infections in  
502 patients with AIDS: report of five cases and review. *Rev Infect Dis.* 1991;13(3):413-7.
- 503 20. Hung CC, Hung MN, Hsueh PR, Chang SY, Chen MY, Hsieh SM, et al. Risk of recurrent  
504 nontyphoid *Salmonella* bacteremia in HIV-infected patients in the era of highly active  
505 antiretroviral therapy and an increasing trend of fluoroquinolone resistance. *Clin Infect Dis.*  
506 2007;45(5):e60-7.
- 507 21. Kales CP, Holzman RS. Listeriosis in patients with HIV infection: clinical manifestations  
508 and response to therapy. *J Acquir Immune Defic Syndr (1988).* 1990;3(2):139-43.
- 509 22. Levine MM, Farag TH. Invasive salmonella infections and HIV in Northern Tanzania. *Clin*  
510 *Infect Dis.* 2011;52(3):349-51.
- 511 23. WHO. Global Tuberculosis Report 2016. 2016.
- 512 24. Flannagan RS, Cosio G, Grinstein S. Antimicrobial mechanisms of phagocytes and  
513 bacterial evasion strategies. *Nat Rev Microbiol.* 2009;7(5):355-66.
- 514 25. Weiss G, Schaible UE. Macrophage defense mechanisms against intracellular bacteria.  
515 *Immunol Rev.* 2015;264(1):182-203.
- 516 26. Harty JT, Bevan MJ. Specific immunity to *Listeria monocytogenes* in the absence of IFN  
517 gamma. *Immunity.* 1995;3(1):109-17.
- 518 27. Bao S, Beagley KW, France MP, Shen J, Husband AJ. Interferon-gamma plays a critical  
519 role in intestinal immunity against *Salmonella typhimurium* infection. *Immunology.*  
520 2000;99(3):464-72.
- 521 28. Kawakami K, Kinjo Y, Uezu K, Miyagi K, Kinjo T, Yara S, et al. Interferon-gamma  
522 production and host protective response against *Mycobacterium tuberculosis* in mice lacking  
523 both IL-12p40 and IL-18. *Microbes Infect.* 2004;6(4):339-49.
- 524 29. Bellamy R. Susceptibility to mycobacterial infections: the importance of host genetics.  
525 *Genes Immun.* 2003;4(1):4-11.
- 526 30. Liu PT, Modlin RL. Human macrophage host defense against *Mycobacterium*  
527 *tuberculosis*. *Curr Opin Immunol.* 2008;20(4):371-6.
- 528 31. Nairz M, Fritsche G, Brunner P, Talasz H, Hantke K, Weiss G. Interferon-gamma limits  
529 the availability of iron for intramacrophage *Salmonella typhimurium*. *Eur J Immunol.*  
530 2008;38(7):1923-36.

- 531 32. Gomes MS, Dom G, Pedrosa J, Boelaert JR, Appelberg R. Effects of iron deprivation on  
532 *Mycobacterium avium* growth. *Tuber Lung Dis.* 1999;79(5):321-8.
- 533 33. Haschka D, Nairz M, Demetz E, Wienerroither S, Decker T, Weiss G. Contrasting  
534 regulation of macrophage iron homeostasis in response to infection with *Listeria*  
535 *monocytogenes* depending on localization of bacteria. *Metallomics.* 2015;7(6):1036-45.
- 536 34. Nugent SL, Meng F, Martin GB, Altier C. Acquisition of Iron Is Required for Growth of  
537 *Salmonella* spp. in Tomato Fruit. *Appl Environ Microbiol.* 2015;81(11):3663-70.
- 538 35. Siegrist MS, Unnikrishnan M, McConnell MJ, Borowsky M, Cheng TY, Siddiqi N, et al.  
539 *Mycobacterial* Esx-3 is required for mycobactin-mediated iron acquisition. *Proc Natl Acad Sci U*  
540 *S A.* 2009;106(44):18792-7.
- 541 36. De Voss JJ, Rutter K, Schroeder BG, Su H, Zhu Y, Barry CE, 3rd. The salicylate-derived  
542 mycobactin siderophores of *Mycobacterium tuberculosis* are essential for growth in  
543 macrophages. *Proc Natl Acad Sci U S A.* 2000;97(3):1252-7.
- 544 37. Khan FA, Fisher MA, Khakoo RA. Association of hemochromatosis with infectious  
545 diseases: expanding spectrum. *Int J Infect Dis.* 2007;11(6):482-7.
- 546 38. Nairz M, Fritsche G, Crouch ML, Barton HC, Fang FC, Weiss G. Slc11a1 limits  
547 intracellular growth of *Salmonella enterica* sv. Typhimurium by promoting macrophage immune  
548 effector functions and impairing bacterial iron acquisition. *Cell Microbiol.* 2009;11(9):1365-81.
- 549 39. Abreu R, Quinn F, Giri PK. Role of the hepcidin-ferroportin axis in pathogen-mediated  
550 intracellular iron sequestration in human phagocytic cells. *Blood Adv.* 2018;2(10):1089-100.
- 551 40. Cassat JE, Skaar EP. Iron in infection and immunity. *Cell Host Microbe.* 2013;13(5):509-  
552 19.
- 553 41. Kontoghiorghes GJ, Kolnagou A, Skiada A, Petrikkos G. The role of iron and chelators  
554 on infections in iron overload and non iron loaded conditions: prospects for the design of new  
555 antimicrobial therapies. *Hemoglobin.* 2010;34(3):227-39.
- 556 42. Cronje L, Edmondson N, Eisenach KD, Bornman L. Iron and iron chelating agents  
557 modulate *Mycobacterium tuberculosis* growth and monocyte-macrophage viability and effector  
558 functions. *FEMS Immunol Med Microbiol.* 2005;45(2):103-12.
- 559 43. Boehm U, Klamp T, Groot M, Howard JC. Cellular responses to interferon-gamma. *Annu*  
560 *Rev Immunol.* 1997;15:749-95.
- 561 44. Schoenborn JR, Wilson CB. Regulation of interferon-gamma during innate and adaptive  
562 immune responses. *Adv Immunol.* 2007;96:41-101.
- 563 45. Nemeth E, Tuttle MS, Powelson J, Vaughn MB, Donovan A, Ward DM, et al. Hepcidin  
564 regulates cellular iron efflux by binding to ferroportin and inducing its internalization. *Science.*  
565 2004;306(5704):2090-3.
- 566 46. Pamer EG. Immune responses to *Listeria monocytogenes*. *Nat Rev Immunol.*  
567 2004;4(10):812-23.

- 568 47. Moreira AC, Neves JV, Silva T, Oliveira P, Gomes MS, Rodrigues PN. Hepcidin-  
569 (In)dependent Mechanisms of Iron Metabolism Regulation during Infection by *Listeria* and  
570 *Salmonella*. *Infect Immun*. 2017;85(9).
- 571 48. Abreu R, Essler L, Loy A, Quinn F, Giri P. Heparin inhibits intracellular *Mycobacterium*  
572 tuberculosis bacterial replication by reducing iron levels in human macrophages. *Sci Rep*.  
573 2018;8(1):7296.
- 574 49. Xu M, Kashanchi F, Foster A, Rotimi J, Turner W, Gordeuk VR, et al. Heparin induces  
575 HIV-1 transcription inhibited by ferroportin. *Retrovirology*. 2010;7:104.
- 576 50. Brosch R, Gordon SV, Garnier T, Eiglmeier K, Frigui W, Valenti P, et al. Genome  
577 plasticity of BCG and impact on vaccine efficacy. *Proc Natl Acad Sci U S A*. 2007;104(13):5596-  
578 601.
- 579 51. Gunawardena HP, Feltcher ME, Wrobel JA, Gu S, Braunstein M, Chen X. Comparison  
580 of the membrane proteome of virulent *Mycobacterium tuberculosis* and the attenuated  
581 *Mycobacterium bovis* BCG vaccine strain by label-free quantitative proteomics. *J Proteome*  
582 *Res*. 2013;12(12):5463-74.
- 583 52. Trivedi NH, Yu JJ, Hung CY, Doelger RP, Navara CS, Armitage LY, et al. Microbial co-  
584 infection alters macrophage polarization, phagosomal escape, and microbial killing. *Innate*  
585 *Immun*. 2018;24(3):152-62.
- 586 53. Chavez-Galan L, Vesin D, Martinvalet D, Garcia I. Low Dose BCG Infection as a Model  
587 for Macrophage Activation Maintaining Cell Viability. *J Immunol Res*. 2016;2016:4048235.
- 588 54. Alli OA, Ogbolu DO, Spreadbury CL. Development of infection model for studying  
589 intracellular gene expression of *Mycobacterium tuberculosis*. *Afr J Med Med Sci*.  
590 2009;38(4):325-32.
- 591 55. Chlosta S, Fishman DS, Harrington L, Johnson EE, Knutson MD, Wessling-Resnick M,  
592 et al. The iron efflux protein ferroportin regulates the intracellular growth of *Salmonella enterica*.  
593 *Infect Immun*. 2006;74(5):3065-7.
- 594 56. Jellbauer S, Perez Lopez A, Behnsen J, Gao N, Nguyen T, Murphy C, et al. Beneficial  
595 Effects of Sodium Phenylbutyrate Administration during Infection with *Salmonella enterica*  
596 Serovar Typhimurium. *Infect Immun*. 2016;84(9):2639-52.
- 597 57. Sheldon JR, Laakso HA, Heinrichs DE. Iron Acquisition Strategies of Bacterial  
598 Pathogens. *Microbiol Spectr*. 2016;4(2).
- 599 58. Sritharan M. Iron Homeostasis in *Mycobacterium tuberculosis*: Mechanistic Insights into  
600 Siderophore-Mediated Iron Uptake. *J Bacteriol*. 2016;198(18):2399-409.
- 601 59. Hameed S, Pal R, Fatima Z. Iron Acquisition Mechanisms: Promising Target Against  
602 *Mycobacterium tuberculosis*. *Open Microbiol J*. 2015;9:91-7.
- 603 60. Luo M, Fadeev EA, Groves JT. Mycobactin-mediated iron acquisition within  
604 macrophages. *Nat Chem Biol*. 2005;1(3):149-53.



- 605 61. Surguladze N, Patton S, Cozzi A, Fried MG, Connor JR. Characterization of nuclear  
606 ferritin and mechanism of translocation. *Biochem J.* 2005;388(Pt 3):731-40.
- 607 62. Buchmeier NA, Heffron F. Inhibition of macrophage phagosome-lysosome fusion by  
608 *Salmonella typhimurium*. *Infect Immun.* 1991;59(7):2232-8.
- 609 63. Ong ST, Ho JZ, Ho B, Ding JL. Iron-withholding strategy in innate immunity.  
610 *Immunobiology.* 2006;211(4):295-314.
- 611 64. Hantke K, Nicholson G, Rabsch W, Winkelmann G. Salmochelins, siderophores of  
612 *Salmonella enterica* and uropathogenic *Escherichia coli* strains, are recognized by the outer  
613 membrane receptor IroN. *Proc Natl Acad Sci U S A.* 2003;100(7):3677-82.
- 614 65. Parrow NL, Fleming RE, Minnick MF. Sequestration and scavenging of iron in infection.  
615 *Infect Immun.* 2013;81(10):3503-14.
- 616 66. Lechowicz J, Krawczyk-Balska A. An update on the transport and metabolism of iron in  
617 *Listeria monocytogenes*: the role of proteins involved in pathogenicity. *Biometals.*  
618 2015;28(4):587-603.
- 619 67. Schnupf P, Portnoy DA. Listeriolysin O: a phagosome-specific lysin. *Microbes Infect.*  
620 2007;9(10):1176-87.
- 621 68. Krause A, Neitz S, Magert HJ, Schulz A, Forssmann WG, Schulz-Knappe P, et al.  
622 LEAP-1, a novel highly disulfide-bonded human peptide, exhibits antimicrobial activity. *FEBS*  
623 *Lett.* 2000;480(2-3):147-50.
- 624 69. Park CH, Valore EV, Waring AJ, Ganz T. Hepcidin, a urinary antimicrobial peptide  
625 synthesized in the liver. *J Biol Chem.* 2001;276(11):7806-10.
- 626 70. Arezes J, Jung G, Gabayan V, Valore E, Ruchala P, Gulig PA, et al. Hepcidin-induced  
627 hypoferremia is a critical host defense mechanism against the siderophilic bacterium *Vibrio*  
628 *vulnificus*. *Cell Host Microbe.* 2015;17(1):47-57.
- 629 71. Drakesmith H, Nemeth E, Ganz T. Ironing out Ferroportin. *Cell Metab.* 2015;22(5):777-  
630 87.
- 631 72. Kasvosve I. Effect of ferroportin polymorphism on iron homeostasis and infection. *Clin*  
632 *Chim Acta.* 2013;416:20-5.
- 633 73. De Domenico I, Zhang TY, Koenig CL, Branch RW, London N, Lo E, et al. Hepcidin  
634 mediates transcriptional changes that modulate acute cytokine-induced inflammatory responses  
635 in mice. *J Clin Invest.* 2010;120(7):2395-405.
- 636 74. Nemeth E, Valore EV, Territo M, Schiller G, Lichtenstein A, Ganz T. Hepcidin, a putative  
637 mediator of anemia of inflammation, is a type II acute-phase protein. *Blood.* 2003;101(7):2461-  
638 3.
- 639 75. Sow FB, Alvarez GR, Gross RP, Satoskar AR, Schlesinger LS, Zwilling BS, et al. Role of  
640 STAT1, NF-kappaB, and C/EBPbeta in the macrophage transcriptional regulation of hepcidin by  
641 mycobacterial infection and IFN-gamma. *J Leukoc Biol.* 2009;86(5):1247-58.

642 76. Ross SL, Tran L, Winters A, Lee KJ, Plewa C, Foltz I, et al. Molecular mechanism of  
643 hepcidin-mediated ferroportin internalization requires ferroportin lysines, not tyrosines or JAK-  
644 STAT. *Cell Metab.* 2012;15(6):905-17.

645

## 646 **Supporting information**

647 **S1 Fig. Hepcidin silencing in THP-1 macrophages.** A) Hepcidin secretion in ShHAMP THP-1  
648 macrophages and respective ShScram controls after infection with *M. bovis* BCG, *L.*  
649 *monocytogenes* and *S. enterica*. B) Surface ferroportin expression in ShHAMP THP-1  
650 macrophages and respective ShScram controls measured by flow cytometry.

651 **S2 Fig. *Listeria monocytogenes* downregulates ferroportin by a hepcidin-independent**  
652 **mechanism.** Ferroportin expression in ShHAMP THP-1 macrophages eight hours post-infection  
653 with *L. monocytogenes* and 16 hours post-infection with *S. enterica*. Ferroportin levels were  
654 quantified by mean fluorescence intensity of 40 cells from three different fields of three  
655 independent experiments. \*\*\* $p < 0.001$

656 **S3 Fig. Iron chelation inhibits intracellular bacterial replication.** A) Intracellular iron Prussian  
657 Blue staining in macrophages infected with three siderophilic bacteria. B) Percentage of Prussian  
658 Blue (PB) pixels in THP-1 macrophages after infection with three siderophilic bacteria. (C)  
659 *Mycobacterium tuberculosis* intracellular burden in THP-1 macrophages in presence of iron  
660 chelator DFO. D) *Listeria monocytogenes* intracellular burden in THP-1 macrophages in  
661 presence of iron chelator DFP. E) *Salmonella enterica* intracellular burden in THP-1 macrophages  
662 in presence of iron chelator DFP. \*\* $p < 0.01$ , \*\*\* $p < 0.001$ . All data were from three independent  
663 experiments.

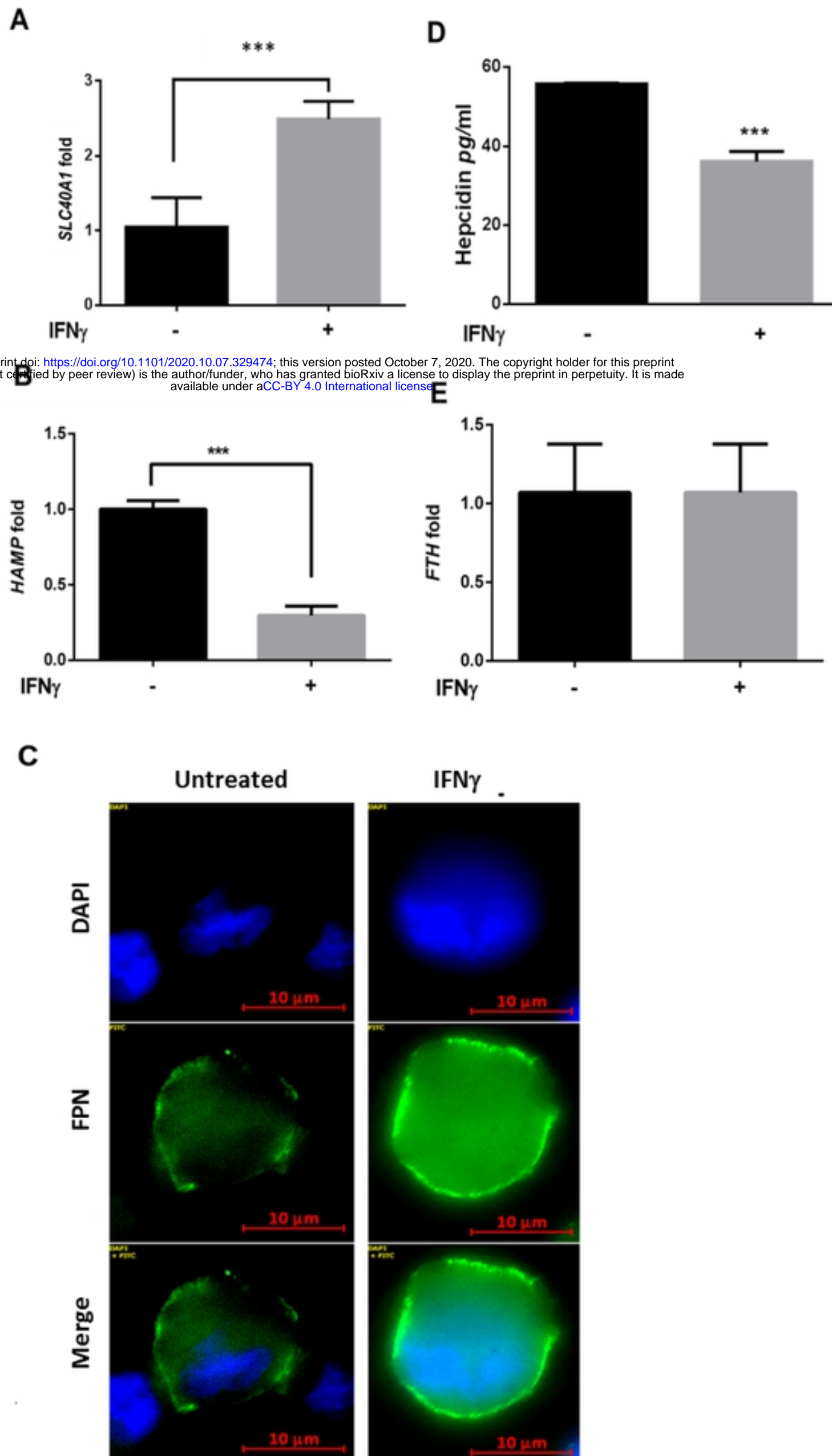
664 **S4 Fig. Interferon-gamma induces ferroportin expression after *Listeria monocytogenes***  
665 **bacterial infection.** Ferroportin in IFN- $\gamma$ -treated THP-1 macrophages eight hours post-infection

666 with *L. monocytogenes*, 16 hours post-infection with *S. enterica* and 24 hours post-infection with  
667 *M. bovis* BCG bacteria. Ferroportin levels were quantified by mean fluorescence intensity of 40  
668 cells from three different fields of three independent experiments. \* $p < 0.05$ , \*\*\* $p < 0.001$ .

669 **S5 Fig. Iron impacts intracellular replication of siderophilic bacteria in macrophages.** A)  
670 THP-1 macrophages differentiated as described in Materials and Methods, rested and infected in  
671 iron-supplemented medium. *Listeria monocytogenes* (A) and *S. enterica* (B) intracellular bacterial  
672 burdens were determined by a gentamicin protection assay. \*\*\* $p < 0.001$ . Data were from three  
673 independent experiments.

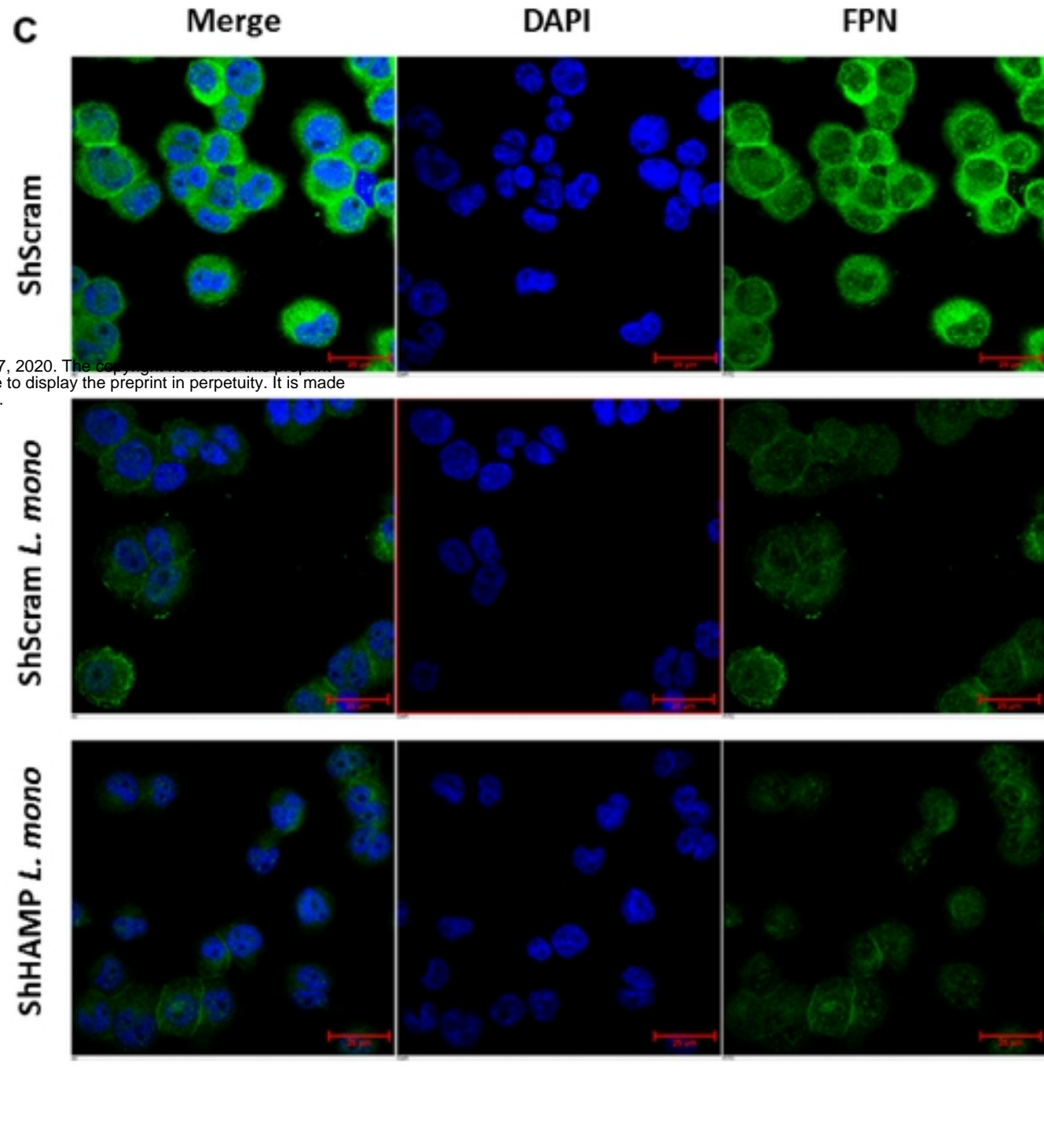
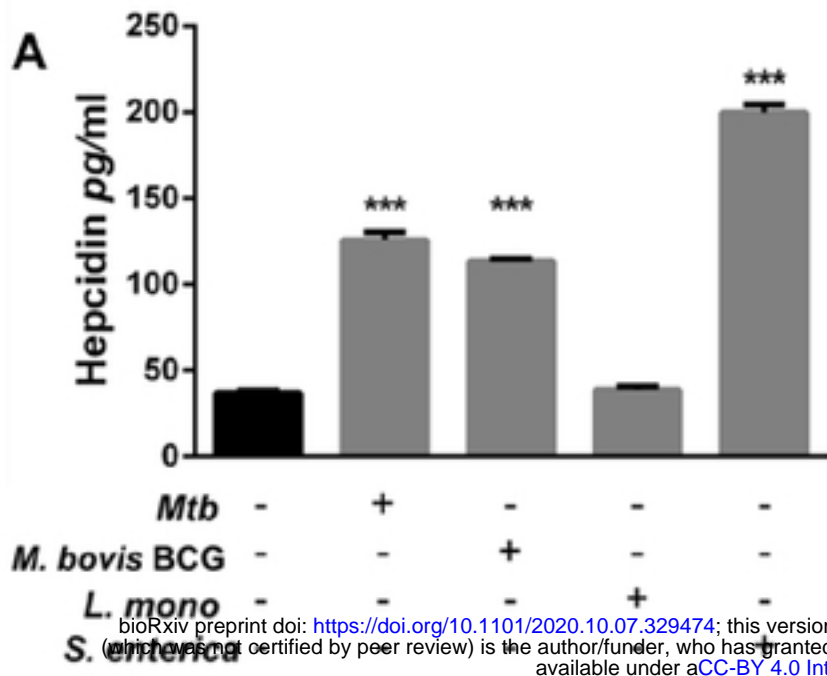
674 **S6 Fig. Hepcidin silencing decreases intracellular *Mycobacterium bovis* BCG replication.**  
675 *Mycobacterium bovis* BCG intracellular burden in ShHAMP THP-1 macrophages 24 hours post-  
676 infection. \*\* $p < 0.01$ . Data were from three independent experiments.

Fig. 1



bioRxiv preprint doi: <https://doi.org/10.1101/2020.10.07.329474>; this version posted October 7, 2020. The copyright holder for this preprint (which was not certified by peer review) is the author/funder, who has granted bioRxiv a license to display the preprint in perpetuity. It is made available under aCC-BY 4.0 International license.

Fig. 2



bioRxiv preprint doi: <https://doi.org/10.1101/2020.10.07.329474>; this version posted October 7, 2020. The copyright holder for this preprint (which was not certified by peer review) is the author/funder, who has granted bioRxiv a license to display the preprint in perpetuity. It is made available under aCC-BY 4.0 International license.

Fig. 3

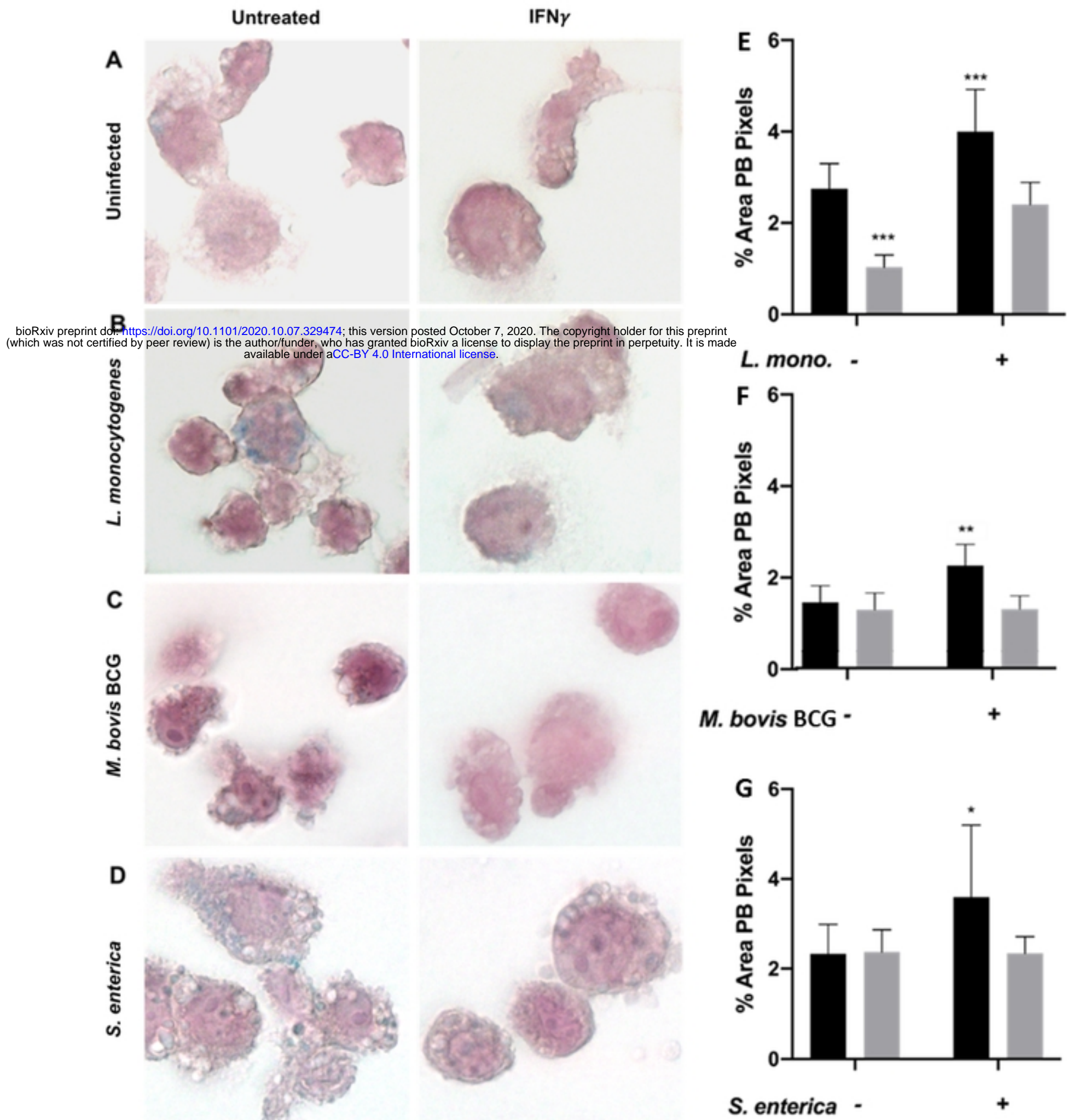


Fig. 4

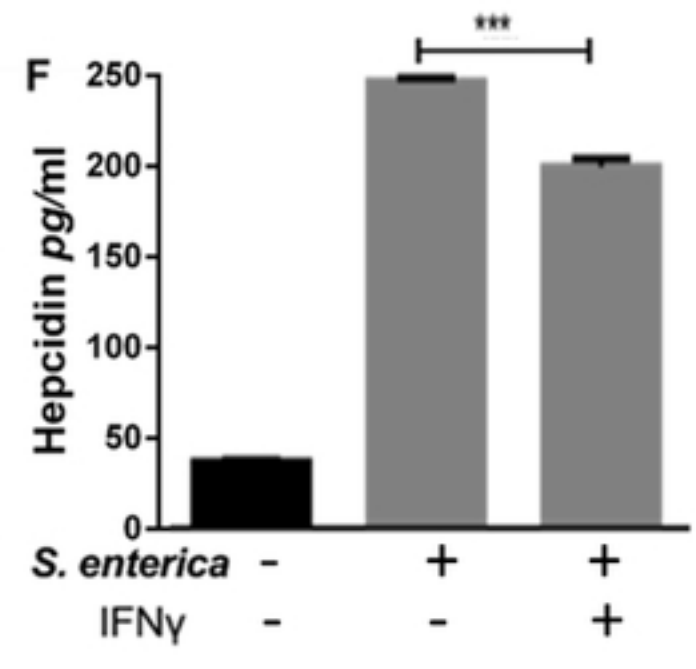
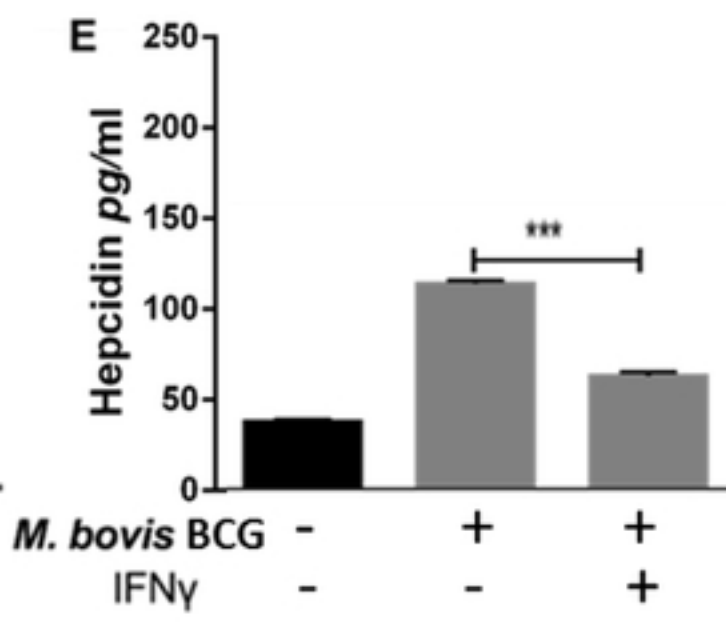
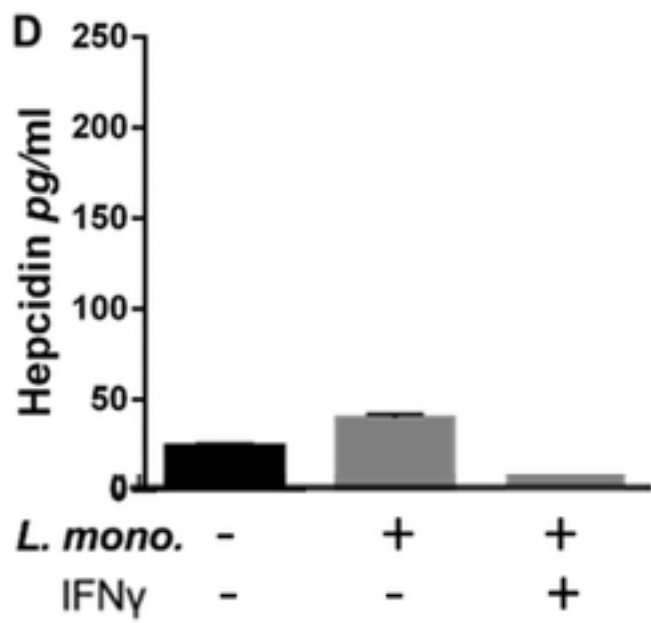
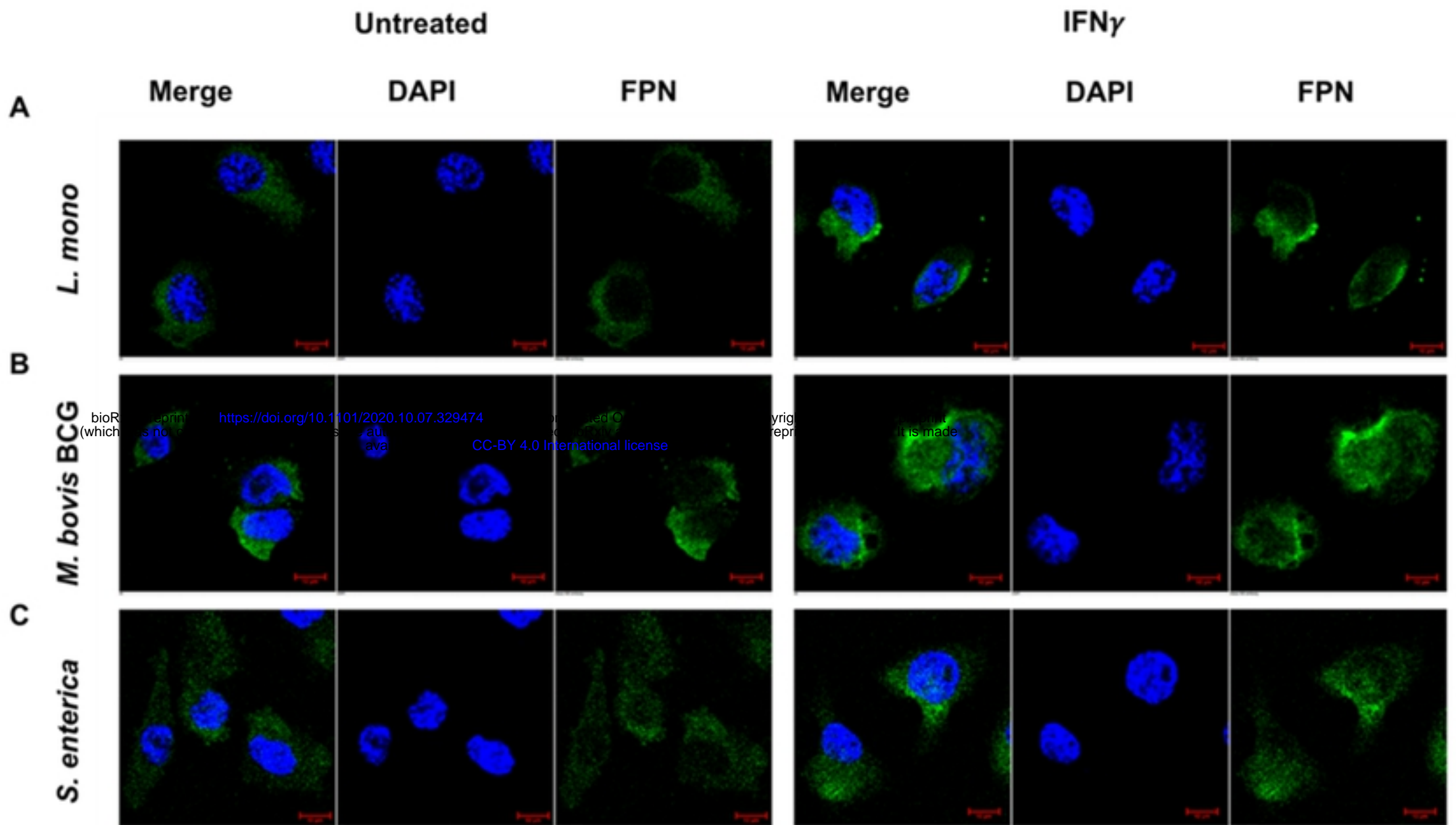


Fig. 5

